### **Article**

# SEMA3A Signaling Controls Layer-Specific Interneuron Branching in the Cerebellum

Jean-Michel Cioni, <sup>1,2,3</sup> Ludovic Telley, <sup>1,2,3</sup> Véronique Saywell, <sup>1,2,3</sup> Christelle Cadilhac, <sup>1,2,3</sup> Carole Jourdan, <sup>1,2,3</sup> Andrea B. Huber, <sup>4</sup> Josh Z. Huang, <sup>5</sup> Céline Jahannault-Talignani, <sup>1,2,3</sup> and Fabrice Ango <sup>1,2,3,\*</sup> <sup>1</sup>CNRS, UMR5203, Department of Neurobiology, Institut de Génomique Fonctionnelle, 34094 Montpellier, France <sup>2</sup>INSERM, U661, 34094 Montpellier, France <sup>3</sup>Université de Montpellier 1 and 2, 34094 Montpellier, France <sup>4</sup>Institute of Developmental Genetics, Helmholtz Zentrum München, German Research Center for Environmental Health, 85764 Neuherberg, Germany <sup>5</sup>Cold Spring Harbor Laboratory, Cold Spring Harbor, NY 11724, USA

#### Summary

**Background:** GABAergic interneurons regulate the balance and dynamics of neural circuits, in part, by elaborating their strategically placed axon branches that innervate specific cellular and subcellular targets. However, the molecular mechanisms that regulate target-directed GABAergic axon branching are not well understood.

Results: Here we show that the secreted axon guidance molecule, SEMA3A, expressed locally by Purkinje cells, regulates cerebellar basket cell axon branching through its cognate receptor Neuropilin-1 (NRP1). SEMA3A was specifically localized and enriched in the Purkinje cell layer (PCL). In sema3A<sup>-/-</sup> and nrp1<sup>sema-/sema-</sup> mice lacking SEMA3A-binding domains, basket axon branching in PCL was reduced. We demonstrate that SEMA3A-induced axon branching was dependent on local recruitment of soluble guanylyl cyclase (sGC) to the plasma membrane of basket cells, and sGC subcellular trafficking was regulated by the Src kinase FYN. In fyn-deficient mice, basket axon terminal branching was reduced in PCL, but not in the molecular layer.

**Conclusions:** These results demonstrate a critical role of local SEMA3A signaling in layer-specific axonal branching, which contributes to target innervation.

#### Introduction

The establishment of specific neuronal connectivity often involves sequential and coordinated steps, including cell migration, axon growth and guidance to their target area, terminal branching within the target domains, and synapse formation [1–5]. Like axon guidance, axon branching is tightly regulated to establish specific neural connectivity. The temporal and spatial control of branching is crucial during circuit development and confers characteristic morphology on each neuronal cell type. Specific and regulated axon branching may also contribute to target selection and structural plasticity [6–8].

An axonal branch can form through at least three distinct modes: (1) bifurcation of a growth cone, (2) collateral

branching from the axon shaft, and (3) terminal branching. Distinct axonal branching is well exemplified by GABAergic interneurons in the neocortex. Indeed, differential classes of interneurons extend axon arbors that are vertical, horizontal, or laminated and thereby distribute their output to the same or multiple layers and columns [9–11]. In addition, most interneuron axons have exuberant local branching, with which they seek out specific cell types and impose strong control over local neuron populations [12, 13]. Despite its functional importance, the molecular mechanisms that regulate precise axonal branching of GABAergic interneurons are unclear.

In the cerebellar cortex, the Purkinje cells receive two sets of inhibitory GABAergic inputs from molecular layer interneurons. The stellate cell selectively innervates the Purkinje cell dendritic shaft, whereas the basket cell targets the Purkinje soma and axon initial segment (AIS). Each interneuron type displays a unique axon organization and branching pattern. For example, basket axons first form several collateral branchings that innervate Purkinje cells, and each collateral displays abundant local terminal branches at the Purkinje soma and AIS to form the pinceau synapse [14]. Whether these different modes of branching are regulated by a cell-type-intrinsic program [15] or by extracellular cues remains an open question. In the present study, we identify the secreted axon guidance molecule semaphorin-3A (SEMA3A) and associated signaling pathway as key regulators of basket cell axon branching that likely contribute to specific synapse formation with Purkinje cells at the axon initial segment.

#### Results

Terminal Basket Axon Branching Is Reduced in  $sema3A^{-/-}$  and  $nrp1^{sema-/sema-}$ 

The formation of the pinceau at the Purkinje hillock was previously described [16, 17]. The mature brush-shaped synapse labeled with parvalbumin (Parv) antibody at P21 (Figure 1A) consisted of multiple axon terminal branching that occurred exclusively in the Purkinje cell layer (PCL). This branching pattern was observed by using bacterial artificial chromosome (BAC) transgenic mice labeling single basket cells with GFP (Figure 1B) [18]. Notably, in the molecular layer (ML), axon collaterals were relatively simple with very few or no branches, whereas in the PCL, they made several branches that terminated around the soma and AIS of Purkinje cells. However, the cellular and molecular mechanisms that controlled this specific layer-branching pattern remained completely unknown.

In situ hybridization showed that *Sema3A* mRNA was detected in all Purkinje cells by P10 [19]. In mice deficient for SEMA3A, cerebellar organization was unchanged, and most cerebellar projections developed normally [20]. On the other hand, the function of long-range axon guidance SEMA3A on local interneuron axon development remains unknown. Here, we analyzed basket axon branching at Purkinje AIS in *sema3A*<sup>-/-</sup>. To this end, the width of pinceau synapses was measured after its specific labeling with Parv antibody (Figure 1C). Indeed, we found that the width of the pinceau synapse showed a direct correlation with the terminal branch



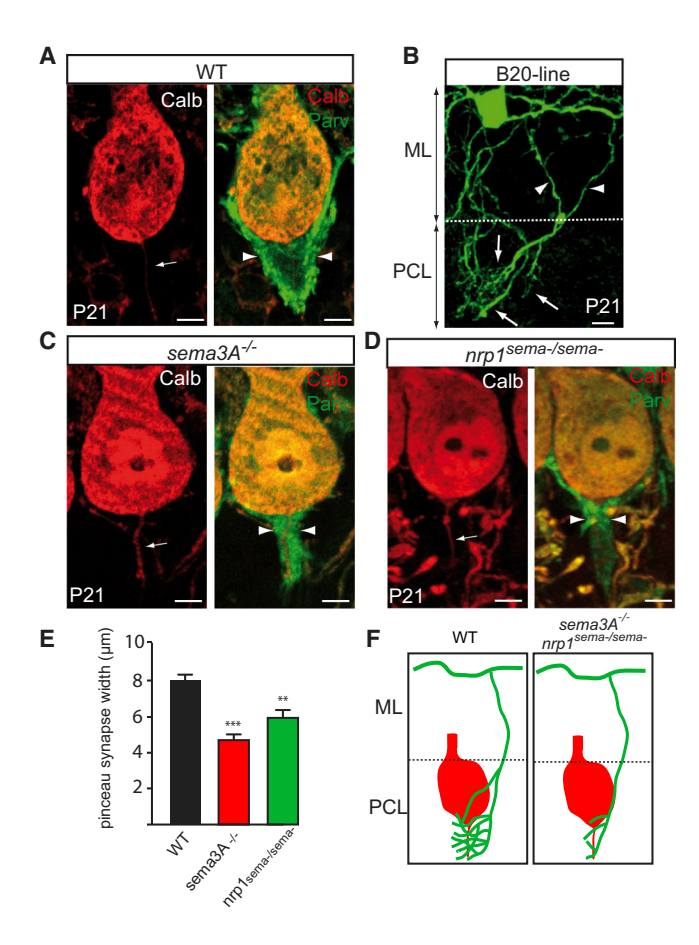


Figure 1. Knockdown of SEMA3A or NRP1<sup>sema-/sema-</sup> Disrupted Basket Axon Terminal Branching and Pinceau Synapses

(A) Cerebellar sections at P21 immunostained against parvalbumin (Parv) and calbindin (Calb) to respectively labeled GABAergic interneurons and Purkinje cells in wild-type mice (WT). Arrows indicate Purkinje axon, and arrowhead highlights pinceau synapse width.

(B) Example of sagittal sections of Parv-GFP (B20 line) cerebellum, in which GFP was expressed in sparse basket cells. Dotted lines represent the Purkinje cell layer (PCL). ML, molecular layer. Arrows show axonal branching in PCL compared to arrowhead in ML.

(C and D) Cerebellar sections at P21 immunostained against parvalbumin (Parv) and calbindin (Calb) in  $sema3A^{-/-}$  (C) and  $nrp1^{sema-/sema-}$  (D). Arrows indicate Purkinje axon, and arrowhead points to the pinceau synapse width. Note that the cone shape of the pinceau synapse was reduced in  $sema3A^{-/-}$  and  $nrp1^{sema-/sema-}$  compared to WT.

(E) Quantification of pinceau synapse width ( $\mu$ m) in WT (8.02  $\pm$  0.36; n = 12 from four WT mice), se $ma3A^{-/-}$  (4.69  $\pm$  0.29; n = 12 from three mutant mice), and  $nrp1^{sema-/sema-}$  (5.9  $\pm$  0.42; n = 19 from three mutant mice).

(F) Schematic representation of basket axon branching. Primary axon collaterals emerged from the axon shaft in ML and branched profusely only in PCL in WT, but not in sema3A<sup>-/-</sup> and nrp1<sup>sema-/sema</sup>.

Error bars represent SEM. \*\*p < 0.005, \*\*\*p < 0.001; Mann-Whitney test. In (A)–(D), scale bars represent 5  $\mu$ m.

formation of GABAergic axons that occurred during cerebellar development (see Figure S1 available online). Our analysis at P21 revealed a significant decrease of pinceau synapses in sema3A<sup>-/-</sup> (Figure 1C). We observed a nearly 50% reduction of the width of the synapses, suggesting reduced basket axon branching (Figure 1E).

To determine whether SEMA3A function was transduced by receptor complexes composed with the obligate ligand-binding component Neuropilin-1 (NRP1) [21, 22], we quantified pinceau synapses in *nrp1*<sup>sema-/sema-</sup> mutant mice that lack a

functional semaphorin-binding domain [23] (Figure 1D). In  $nrp1^{sema-/sema-}$  mice, we observed a significant reduction of the size of the pinceau synapse as quantified in Figure 1E. The reduced pinceau synapse width observed in  $sema3A^{-/-}$  and  $nrp1^{sema-/sema-}$  (Figure 1F) might reflect a direct function of SEMA3A on basket axon branch formation or maintenance. However, we cannot exclude an indirect role of SEMA3A in modulating activity-dependent basket axonal remodeling [24].

### SEMA3A-Induced GABAergic Axonal Branching Depends on Neuropilin-1

To investigate whether SEMA3A directly controls GABAergic axon branching, we used a primary culture of cerebellar interneurons from Gad67-GFP transgenic mice [17]. GABAergic interneurons were cocultured in the presence of Chinese hamster ovary (CHO) cells expressing either SEMA3A-Tomato or Tomato as a control. After 1 day in vitro (DIV1), GFP-labeled interneurons were traced, and their morphologies were analyzed using Imaris software (Figure 2A). In the presence of SEMA3A, we observed an increase in axonal branches as compared to the control condition (Figure 2B). The effect of SEMA3A on GABAergic axons was specific, given that analysis of the dendritic branching revealed no difference between SEMA3A-treated and control neurons (Figure 2C). To further characterize the branching pattern, we analyzed the axon arbor complexity using the axonal complexity index (ACI), which takes into account the number of branches of different orders [25] (Figure 2D). The average ACI value was significantly higher in SEMA3A-treated neurons as compared to control neurons (Figure 2D). In control neurons, the axon morphology was simple and mainly composed of an axon branch order of 1. In the presence of SEMA3A, we observed an increased number of branch orders greater than 1, suggesting that its major action was to contribute to GABAergic axon branch terminal complexity.

Next, we asked whether SEMA3A-induced GABAergic axon branching depended on its canonical receptor containing NRP1, as suggested in vivo. We first evaluated the expression and localization of endogenous NRP1 and its classical coreceptor plexinA1 on GABAergic interneuron primary culture using both western blot and immunohistochemistry. We found that NRP1 and plexinA1 were expressed by GABAergic interneurons and localized on the axonal growth cone after 1 day in vitro (Figure S2). SEMA3A function was then studied in the presence of blocking antibodies directed against the ectodomain of NRP1 [21, 22, 26]. Under this condition, axons remained relatively simple, and SEMA3A was neither able to increase the number of axonal branches nor the ACI (Figures 2B and 2D). The lack of response of GABAergic interneurons was not due to the antibody per se, because nonimmune antibodytreated neurons remained responsive to SEMA3A (data not shown). Thus, GABAergic axon branching was most likely mediated through activation of the NRP1-containing receptor located in the GABAergic axonal growth cone.

## Local GABAergic Axon Branching Is Instructed by SEMA3A Expression Pattern

It was previously shown, using a coculture model and mathematical assessment, that transfected cells secreted diffusible proteins that could create a local concentration gradient for up to 48 hr [27]. Interestingly, in our model, we noted that most branching occurred close to the CHO cell expressing SEMA3A. To quantitatively assess this observation, we analyzed axon branch distribution by a double Sholl analysis

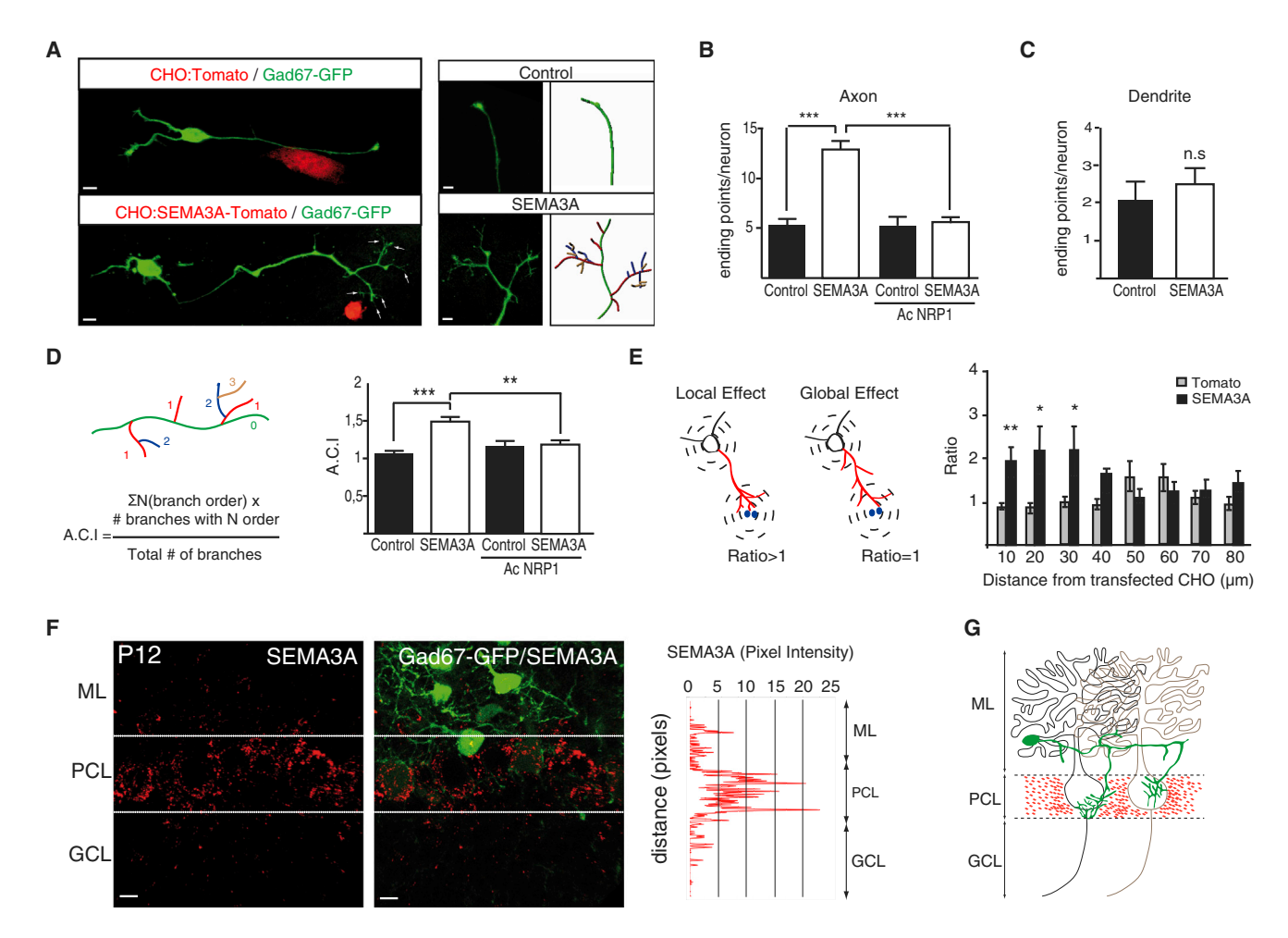


Figure 2. Local GABAergic Axon Branching Was Instructed by SEMA3A Gradient

- (A) Examples of GFP-labeled cerebellar interneurons from Gad67-GFP mice cultured with CHO transfected with semaphorin-3A-Tomato or Tomato. Right panels show higher magnification of axonal terminal complexity and morphological analysis using Imaris software.
- (B) Quantification of axonal ending points (shown as means, n = three cultures). SEMA3A induces an increase in the number of branches (13.07  $\pm$  0.8; n = 27) compared to the control (5.26  $\pm$  0.66; n = 23). Blocking Neuropilin-1 antibody (Ac NRP1) inhibits the effect of SEMA3A on axonal branching (5.56  $\pm$  0.61; n = 16). (C) SEMA3A has no effect on dendritic branches.
- (D) Formula for the axonal complexity index, adapted from Marshak et al. [25]. Graph shows the average axon complexity index value per axon arbor. SEMA3A increases the complexity of GABAergic axon (1.51  $\pm$  0.05; n = 27) compared to the control (1.08  $\pm$  0.03; n = 23) in a NRP1-dependent manner (1.19  $\pm$  0.07; n = 16).
- (E) Schematic representation of the double Sholl analysis applied to interneurons. Blue dots represent CHO cells. Quantification of the ratio between the axonal complexity around the CHO cell and around the cell body of the interneuron (right panel). Note that the complexity of interneuron axons was increased exclusively close to the CHO expressing SEMA3A.
- (F) Proximity ligation assay obtained with SEMA3A antibodies on P12 cerebellar sagittal sections from Gad67-GFP mice. Plot profile (ImageJ) of SEMA3A signal in cerebellar cortex layers revealed a high concentration in the PCL.
- (G) Schematic representation of SEMA3A local enrichment in the Purkinje cell layer (PCL). ML, molecular layer; GCL, granule cell layer.

Scale bars represent 4 μm (left panels in A), 3 μm (right panels in A), or 5 μm (in F). Error bars represent SEM. n.s., not significant; \*p < 0.05, \*\*p < 0.005, \*\*\*p < 0.001; Mann-Whitney test.

(Figure 2E). The first Sholl analysis was centered on the GABAergic interneuron soma and gave information about the distribution of axon branches along the axon shaft. The second Sholl analysis was centered on the CHO cell, expressing SEMA3A-T or Tomato, to assess the complexity of the axon branch locally. We then made a ratio between the local Sholl and the Sholl from neuronal soma to quantify the global branch organization. Sholl analyses of the axonal arbors revealed a significant increase in branch number at distances of 10–30  $\mu$ m from the CHO cell expressing SEMA3A (Figure 2E). On the other end, the axonal complexity was very similar at a distance greater than 40  $\mu$ m for neurons that

grew either in the presence of SEMA3A or Tomato (Figure 2E). Thus, Sholl ratio analysis showed that increased axon branching occurred preferentially close to CHO cells expressing SEMA3A, but not homogenously along the axon, suggesting that the gradient of SEMA3A could instruct axon local branching.

The role of the axon guidance gradient has long been inferred in vivo, but relatively few demonstrations of the existence of such local enrichment have been made for secreted molecules. This was mainly due to low expression level of secreted axon guidance molecules or the lack of appropriate signal amplification and detection systems. To overcome

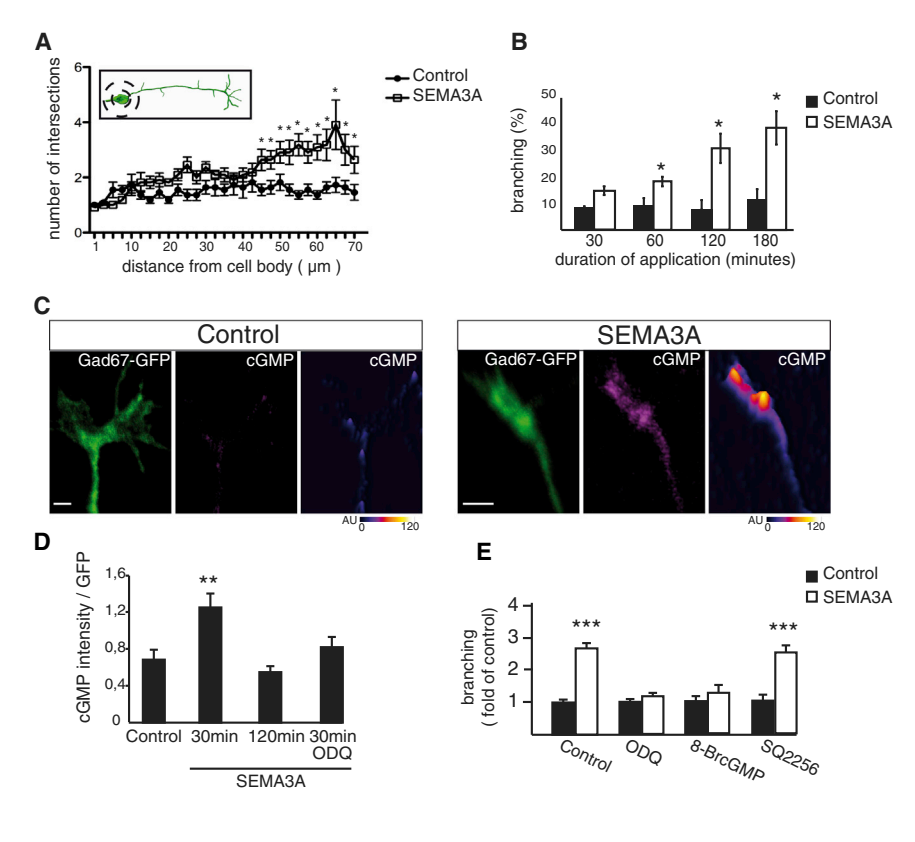


Figure 3. SEMA3A-Induced Local Axonal Branching Was Dependent on sGC Activity

- (A) Schematic representation and quantification of Sholl analysis. Note significant increase of axonal branching in the distal part (last 25  $\mu$ m) after 180 min of SEMA3A treatment.
- (B) Quantification of the percentage of axon terminal branching after application of control or SEMA3A-conditioned medium for 30, 60, 120 or 180 min. Significant increase of axon branching was detected at 60 min (18.34  $\pm$  1.79; n = 589), 120 min (29.79  $\pm$  5.35; n = 592), and 180 min (37.68  $\pm$  6.09; n = 521) after SEMA3A treatment compared to respective controls at 30 min (8.9  $\pm$  0.4; n = 183), 60 min (7.55  $\pm$  2.98; n = 184), and 180 min (11.18  $\pm$  3.55; n = 234).
- (C) Sample images of Gad67-GFP and cGMP immunoreactivity (IR) and cGMP surface plot representation in the GABAergic interneuron growth cone in control and 30 min after SEMA3A application.
- (D) Quantification of cGMP IR in response to SEMA3A normalized to GFP signal. SEMA3A application for 30 min increased cGMP IR from  $0.55\pm0.06$  (n = 14) to  $1.26\pm0.14$  (n = 15), which returned to control level after 120 min of treatment. Inhibition of sGC with ODQ inhibits SEMA3A action (0.83  $\pm$  0.1; n = 13).
- (E) Quantification of axonal branch number shown as fold of control (n = three cultures, 12– 16 cells/condition). Treatment with ODQ and 8-BrcGMP, but not with SQ22536, inhibited the response of SEMA3A on axonal branching.
- Scale bars represent 2  $\mu$ m. Error bars represent SEM. \*p < 0.05, \*\*p < 0.005, \*\*\*p < 0.001; Mann-Whitney test.

these limitations, we used a new methodology called "proximity ligation assay" (PLA), which uses rolling circle amplification for localized detection of proteins or protein interactions in fixed cells or tissues (see Experimental Procedures). With this approach, we obtained a specific signal for SEMA3A that appeared as small dots (Figure 2F; Figure S3). Using acute slices of Gad67-GFP mice at P12, we observed that the signal pattern was restricted in the PCL, and quantification revealed local enrichment of SEMA3A in the PCL (Figure 2F), as schematized in Figure 2G.

## SEMA3A Triggers Terminal GABAergic Axon Branching through Local cGMP Signaling

Our study, both in vitro and in vivo, suggested that local SEMA3A concentration triggered GABAergic axon terminal branch formation. On the other hand, we could not exclude the possibility that SEMA3A also acted on collateral branches sprouting from the axon shaft, as previously observed for netrin [28]. Therefore, we used a time-lapse assay to quantify axon morphology at several time points following SEMA3A acute application by Sholl analysis (Figure 3A). We observed that SEMA3A did not affect the proximal part of GABAergic axons but significantly increased branch formation in the distal part (Figure 3A). Further analysis revealed that SEMA3A specifically acted at the growth cone. Under basal conditions, a significant subset (~75%) of axons had an intact growth cone, and application of control medium had no effect on the growth cone morphology (data not shown). In contrast, application of SEMA3A increased the formation of terminal branches that could be observed as early as 60 min (Figure 3B). Thus, acute and global SEMA3A application acted

preferentially on the GABAergic axon growth cone to produce terminal axon branching.

We therefore hypothesized that SEMA3A signaling might be restricted to the GABAergic growth cone. Indeed, the growth cone is responsible for the integration of multiple extracellular signals and accordingly expresses a large repertoire of receptors in order to fulfill this function [29]. Thus, we investigated if SEMA3A-induced branch formation was dependent on local signaling. One potential reporter of SEMA3A signaling is cGMP. Previous study in retinal ganglion cell (RGC) neurons showed that SEMA3A could induce the local production of cGMP, which was dependent on soluble guanylyl cyclase (sGC) activity [30]. In order to explore this possibility, we sought to analyze the level of cGMP in the GABAergic growth cone, in the presence of SEMA3A, by using a specific and previously characterized cGMP antibody [31, 32]. Because of technical limitations in assessing the intracellular cGMP immunoreactivity (IR), we quantified the change in cGMP level by measuring the ratio between cGMP IR and GFP pixel intensity in the growth cone. In basal conditions, the cGMP signal intensity (mean pixel intensity per unit area) in the growth cone showed a weak expression profile (Figures 3C and 3D). Bath application of SEMA3A induced a transient but significant increase in cGMP signal intensity that peaked at 30 min (Figures 3C and 3D) and returned to basal level after 120 min (Figure 3D). SEMA3Ainduced increase in cGMP was significantly inhibited by application of the sGC inhibitor 1H-[1,2,4]oxadiazole[4,3-α] quinozalin-1-one (ODQ) (Figure 3D). Our result revealed a local modulation of sGC activity by SEMA3A in the interneuron growth cone.

To further assess the implication of cGMP signaling in GABAergic axon branching, we used a pharmacological approach. First, we asked whether increased cGMP level was necessary to induce axon branch formation. ODQ was added to interneuron culture before applying control or SEMA3Aconditioned medium. In the presence of ODQ, SEMA3A was unable to induce axon branching, and neuron morphologies were not different from the control condition (Figure 3E). Second, we asked if a global increase in cGMP level could trigger axon branching. To this end, we treated our culture with the membrane-permeable cGMP analog (8-BrcGMP). Under this condition, SEMA3A positive function in axon branching was completely abolished (Figure 3E). In addition, the inhibition of adenylyl cyclase by SQ22536 did not block the SEMA3A effect (Figure 3E), which argues for a selective cGMP-signaling pathway in the control of GABAergic axon branching. All together, these results indicate that local control of cGMP levels by SEMA3A were necessary for terminal axon branch formation.

### SEMA3A Induces Tyrosine Phosphorylation of sGC $\beta$ 1 Subunit in a FYN-Dependent Manner

How could SEMA3A regulate cGMP level in GABAergic interneurons? One important component to relay many extracellular signals to specific intracellular compartments is tyrosine phosphorylation [33]. Indeed, tyrosine-phosphorylated proteins are enriched at the leading edges of growth cones [34], and a tyrosine kinase inhibitor, K252a, is able to compromise SEMA3A's ability to collapse chicken sensory growth cones [35], hence tyrosine phosphorylation may be part of the SEMA3A signaling pathway. To investigate this issue, we performed phosphotyrosine (pY) immunoprecipitation of GABAergic neuronal extract and compared tyrosine-phosphorylated protein patterns in the presence or absence of SEMA3A. Using western blotting, we demonstrated that at least the 70 kDa isoform of the β1 subunit of sGC was tyrosine-phosphorylated, whereas the α1 subunit remained unphosphorylated on tyrosine (Figure 4A). To further evaluate if the β1 subunit was phosphorylated and not coimmunoprecipitated with other phosphorylated partners, we analyzed the profile of proteins revealed with pY antibody after treatment of the neurons with SEMA3A-conditioned medium. We observed an increase in signal intensity at  $\beta$ 1 apparent molecular weight (70 kDa) and not at α1 subunit molecular weight (80 kDa) (Figure 4A), suggesting that  $\beta$ 1 subunit was indeed phosphorylated on tyrosine in response to SEMA3A stimulation.

Analysis of sGC  $\beta1$  subunit sequence for tyrosine phosphorylation motif revealed the presence of a consensus domain for Src kinases [36]. An antibody directed against this specific phosphorylation site on Tyr192 ( $\beta1$ pY192) has been previously generated [37]. Using this antibody, we found that  $\beta1$ pY192 signals increased in the presence of SEMA3A on GABAergic interneurons (Figure 4B) and was inhibited by the specific Src kinase inhibitor SU6656.

We next asked whether Src kinases were indeed activated by SEMA3A in GABAergic interneurons. Similar experiments using pY immunoprecipitation were peformed to detect two major Src kinases, SRC and FYN. Western blot analysis revealed an increased level of FYN (Figure 4C) and not of SRC phosphorylation (Figure 4D) in SEMA3A stimulated, as compared to the control interneuron. FYN activity can be turned on and off by specific tyrosine phosphorylation. In order to ensure that the increased phosphorylation of FYN corresponded to the active form of the protein, we used an antibody directed against the active form of FYN phosphorylated on

tyrosine 418 (p-FYN). We observed that this specific signal increased in the presence of SEMA3A (Figure 4E). We confirmed these results in a heterologous cell line and showed that tyrosine phosphorylation of  $\beta$ 1 was directly dependent on FYN activity (Figure S4).

### SEMA3A Induces Local Trafficking of sGC to the Plasma Membrane

Our data showed that sGC-increased activity was necessary for the induction of terminal branching by SEMA3A. FYN induced Y192 phosphorylation of the sGC  $\beta$ 1 subunit in a SEMA3A-dependent manner during branch formation. On the other hand, the nonphosphorylatable form of  $\beta$ 1 mutated on Y192 was previously shown to have no effect on sGC activity in a heterologous cell line, suggesting that the phosphorylation per se is not responsible for increased level of cGMP. Interestingly, \( \beta 1 Y 192 \) phosphorylation results in exposition of a docking site for proteins containing SH2 domains, such as Src kinases [37]. And, we confirmed that Y192 phosphorylation was necessary for direct interaction of β1 with FYN in a heterologous system (Figure S5). To further demonstrate that this interaction between FYN and  $\beta1$  occurred in GABAergic interneurons, we performed coimmunoprecipitation experiments in primary culture. Western blot analysis revealed that FYN and  $\beta 1$  interacted specifically and this interaction was enhanced in the presence of SEMA3A (Figure 4F).

What could be the function of such interaction? One key element is that FYN is N-myristoylated and targeted to the plasma membrane [38], where it can constitutively interact with plexinA coreceptors [39]. Moreover, translocation of sGC to the plasma membrane sensitized its enzymatic activity [40]. Therefore, we hypothesized that interaction between FYN and  $\beta$ 1 could induce sGC recruitment to the plasma membrane in a SEMA3A-dependent manner to increase cGMP level. To investigate this possibility, we first showed that FYN and β1 interaction occurred only with active FYN and localized in the plasma membrane compartment in HEK cells (Figure S5). Because this interaction was dependent on β1-Y192 phosphorylation, we then decided to visualize where the phosphorylation of sGC β1 subunit in the presence of SEMA3A occurred by staining cultured interneurons with specific anti-β1pY192 antibody. Confocal microscopic analysis revealed that the growth cone was devoid of signal in the control condition (Figure 4G). On the other hand, 30 min application of SEMA3A induced the appearance of small clusters of sGC β1pY192 immunopositive signals at the edge of filopodia like structures at the distal part of interneuron axons (Figure 4G). Because the GABAergic axon is very thin, it was not possible to observe β1-pY192 signal localization at the plasma membrane. Instead we purified neuronal plasma membrane fractions that were treated with conditioned medium containing SEMA3A or control GFP and evaluated the localization of  $\beta$ 1. In the presence of SEMA3A, we observed an increase in β1 subunit signal in the membrane fraction versus cytoplasmic fraction, as compared to the control condition (Figure 4H). All together, our results showed that β1Y192 phosphorylation by FYN was necessary and sufficient to trigger FYN-β1 association at the plasma membrane in a SEMA3A-dependent manner. These data further suggested that regionalized interaction between FYN and  $\beta$ 1 could locally enhance cGMP.

#### sGC β1Y192 Phosphorylation and Trafficking In Vivo Next, we asked whether the sGC local trafficking mediated by FYN could be observed in the GABAergic interneuron axon at

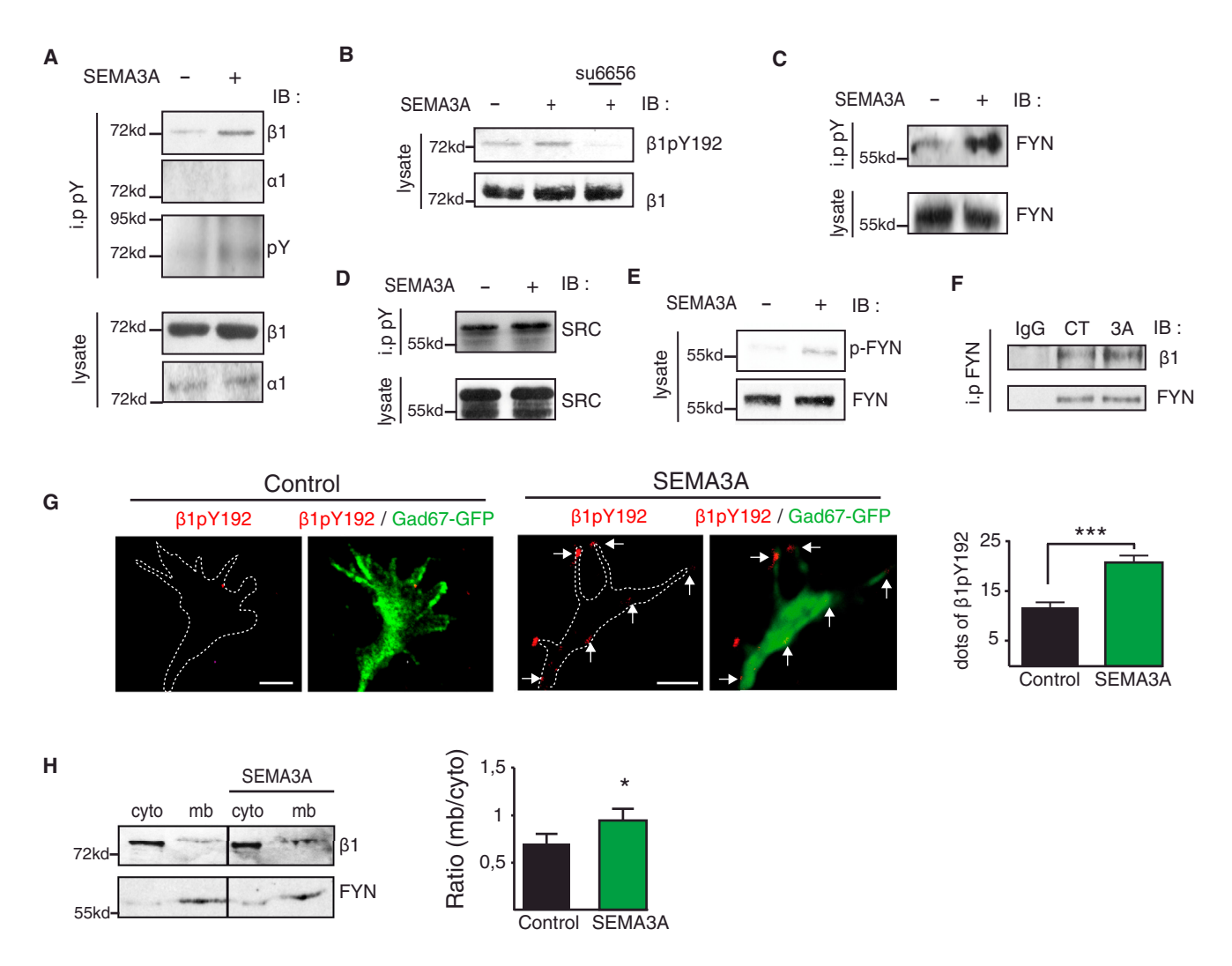


Figure 4. SEMA3A-Stimulated sGC Plasma Membrane Recruitment through FYN Activation

- (A) Immunoprecipitation with anti-phosphotyrosine (pY) was performed on GABAergic interneuron lysate.  $\beta$ 1, but not  $\alpha$ 1, immunoprecipitation with anti-pY is enriched in the presence of SEMA3A (20 min). Note the increased pY band at the molecular weight of  $\beta$ 1 ( $\sim$ 70 kDa), but not of  $\alpha$ 1 ( $\sim$ 80 kDa).
- (B) GABAergic neurons lysates show enriched fraction of β1pY192 in the presence of SEMA3A (20 min) that is inhibited su6656.
- (C and D) FYN, but not Src, immunoprecipitation with anti-pY is enriched in the presence of SEMA3A (20 min).
- (E) p-FYN signal is enriched in the presence of SEMA3A (20 min).
- (F) GABAergic interneuron lysates were immunoprecipitated with anti-FYN after 20 min of stimulation with control (CT) or SEMA3A (3A)-conditioned medium and were immunoblotted with anti-β1 antibody.
- (G) SEMA3A-induced (20 min)  $\beta$ 1pY192 (red) in the GABAergic growth cone (green) as compared to control. Quantification of  $\beta$ 1pY192 clusters (red) in the last 25  $\mu$ m of the axon (green) is shown. \*\*\*p < 0.001; Mann-Whitney test.
- (H) Membrane fraction purification of the GABAergic interneurons stimulated during 20 min with control or SEMA3A and immunoblotted with anti- $\beta$ 1 and FYN antibodies. Quantification of  $\beta$ 1 signal in the membrane as compared to the cytosolic fraction in the presence of control or SEMA3A is seen. i.p., immunoprecipitation; IB, immunoblots. \*p < 0.05; ANOVA test. Scale bars represent 2  $\mu$ m. Error bars represent SEM.

AlS in vivo. Basket cell collaterals reach the Purkinje cell layer at around P8 and start to branch abundantly to finally establish the pinceau synapse at around P16–P21 (Figure 5A). Immunoblot analysis revealed a stable expression of FYN and sGC  $\beta$ 1 between P8 and P21 in cerebellum lysates (Figures 5B and 5C). We next examined p-FYN and  $\beta$ 1pY192 expression at the same stages of development. Immunoprecipitation with anti-FYN and anti- $\beta$ 1 antibody was performed and probed with anti-p-FYN and anti- $\beta$ 1pY192 antibody, respectively. Immunoblot signal for p-FYN was detected at P8 and decreased at subsequent developmental stages (Figure 5B). The time course of  $\beta$ 1pY192 was well correlated with FYN activity (Figure 5C). We next asked if SEMA3A could indeed directly

activate FYN and induce  $\beta$ 1Y192 phosphorylation in acute cerebellar slices. To this end, we first confirmed the expression of NRP1 and plexinA1 in cerebellum at P12 (Figure 5D). In addition, coimmunoprecipitation experiments demonstrated that plexinA1 can associate with Fyn in vivo (Figure 5D). Then, we applied SEMA3A-conditioned medium on cerebellar slices at the same age. We observed a specific increase in both p-FYN and  $\beta$ 1pY192 expression as shown by immunoprecipitation and immunoblot of the respective proteins (Figure 5E).

To reveal the cellular and subcellular localization of the activated signaling pathway, we performed immunohistochemistry experiments of  $\beta$ 1pY192 during cerebellar development. At P12,  $\beta$ 1pY192 signal colocalized with GFP in basket

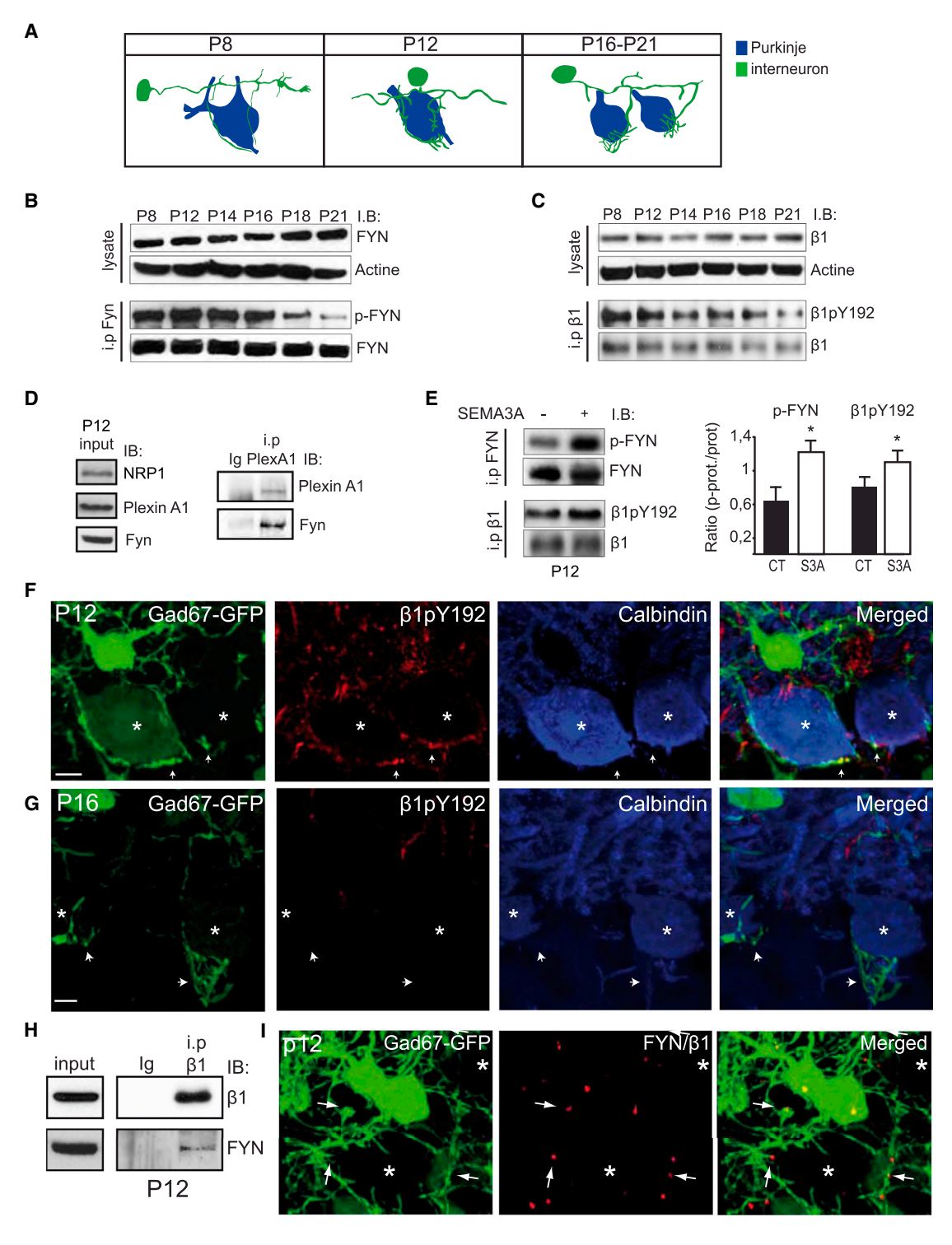


Figure 5. SEMA3A Induced FYN-sGC Signaling in Basket Axon In Vivo

- (A) Schematic representation of basket axon development.
- (B) Whole cerebellar lysates extracted at the indicated stages of development were immunoblotted with anti-FYN and anti-actin (upper two panels) or immunoprecipitated with anti-FYN and immunoblotted with p-FYN (lower two panels).
- (C) Whole cerebellar lysates extracted at the indicated stages of development were immunoblotted with anti- $\beta$ 1 and anti-actin (upper two panels) or immunoprecipitated with anti- $\beta$ 1 antibody and immunoblotted with anti- $\beta$ 1 and anti- $\beta$ 1 pY192 (lower two panels). Note the coincident pattern between p-FYN and  $\beta$ 1 pY192
- (D) Whole cerebellar lysates extracted at P12 were immunoblotted with anti-NRP1, anti-plexinA1, and anti-Fyn antibodies or immunoprecipitated with anti-plexinA1 antibody and immunoblotted with anti-plexinA1 and anti-Fyn.
- (E) Application of SEMA3A (10 min) on P12 slices induced an increase in FYN activation (p-FYN) and β1 phosphorylation as compared to control.

interneurons (Figure 5F). The most intense signal appeared in the terminal axon tip around Purkinje cell soma (Figure 5F). Around P16,  $\beta$ 1pY192 signal disappeared from basket cell axons (Figure 5G), which was correlated with the end of the establishment of the pinceau synapse and axonal branching. Moreover, the absence of  $\beta$ 1pY192 signal at P16 was not due to a lack of  $\beta$ 1, given that its expression could be visualized at P16 at the basket cell pinceau synapse (data not shown).

Finally, FYN- $\beta$ 1 interaction was confirmed by coimmunoprecipitation in vivo at P12 (Figure 5H). To further investigate if this interaction occurred in basket axons, we used the PLA technique, using primary antibodies against FYN and  $\beta$ 1. This method makes it possible to challenge the existence and localization of protein interactions in vitro and in vivo [41]. We performed PLA on slices from Gad67-GFP transgenic mice at P12, and analysis revealed the colocalization of PLA signal with GFP in basket cell axons around Purkinje cell soma (Figure 5I). The signal was specific because it was absent in Gad67-GFP  $\times$  fyn-deficient double-transgenic mice (data not shown). All together, our results showed a local trafficking of sGC in basket cell axons localized in the Purkinje cell layer during cerebellar development.

### Layer-Specific Reduction of GABAergic Axon Branch in FYN Knockout Mice

To further demonstrate that FYN activity was also required for SEMA3A-induced GABAergic axon branching, we first quantified the number of cultured interneuron axon branches in response to SEMA3A alone and in the presence of SU6656. No significant difference was found between control neurons and neurons treated with SEMA3A in the presence of SU6656 (Figure 6B). To further investigate a cell-autonomous function of FYN, expression of FYN was downregulated by nucleofection of specific siRNA. Downregulation of FYN completely abolished the function of SEMA3A in GABAergic interneurons (Figures 6A and 6B).

We next asked whether the FYN signaling pathway was necessary in vivo during basket innervation of the Purkinje axon initial segment (AIS). To test this hypothesis, we analyzed the width of pinceau synapse at P21 in cerebellar slices of wild-type (WT) and *fyn*-deficient mice using confocal microscopy. We showed a drastically diminished pinceau synapse width in *fyn*-/- mice (Figures 6C and 6D), suggesting a decrease in basket cell axon branches at AIS as observed in *sema3A*-/-- and *nrp1*<sup>sema-/sema-</sup>-deficient mice (Figures 1C, 1D, and 1E).

To further demonstrate a specific defect in GABAergic axon terminal branching, we crossed  $fyn^{-/-}$  with BAC transgenic mice that expressed GFP only in a subset of basket interneuron and performed single-cell confocal microscopy analysis [18]. Because expression of GFP in basket cell axon can be detected only after P21, analyzes were performed at later developmental stages. At P40, we observed that in both WT and fyn heterozygote mice, basket cell axon main branching developed parallel to the Purkinje cells, and several ascending collaterals innervated Purkinje soma and AIS, consistent with previous Golgi staining and electromicroscopy analysis [14]. Each collateral further branched at Purkinje AIS to form the pinceau synapse (Figure 6E). The branching pattern of each

axon collateral varied from few to many indistinct branches (Figures 6E and 6F). In  $fyn^{-/-}$ , the overall cell morphology was similar to the control (Figure 6E). Indeed, the main axonal branches grew parallel to the Purkinje cell layer, and the number of axon collaterals developed with no obvious changes in the molecular layer. Strikingly, each axon collateral failed to develop extensive terminal branches at the Purkinje AlS (Figure 6E), which was further quantified in Figure 6F. Basket interneuron branching was altered in  $fyn^{-/-}$ , only in the PCL, thus demonstrating the importance of SEMA3A-FYN signaling in terminal basket cell axon branching in vivo.

#### Discussion

A prominent feature of GABAergic interneurons is the geometry of their axon arbors, which often have multiple side branches that extend with specific trajectories to innervate their targets [42]. Axon branching at specific and strategic locations is a key step in the formation of synaptic connections and local circuitry, but the underlying mechanisms are not well known. In the present study, we examined the role of SEMA3A secreted by targeted-Purkinje cells in basket axon terminal branching in the PCL of the cerebellar cortex. We demonstrated that knocking down SEMA3A or the binding domain of SEMA3A receptor induced a significant reduction of the stereotypical branching pattern of basket axons in PCL. Using a coculture system, we showed that a gradient of SEMA3A induced local terminal branching of GABAergic axons that was dependent on the NRP1 receptor. Furthermore, we showed that SEMA3A triggered the activation of a novel FYN signaling pathway in the axon growth cone that regulates the membrane localization of soluble guanylyl cyclase. Inhibition of sGC or FYN signaling reduced basket axon terminal branching. Knockdown of FYN signaling in vivo specifically reduced stereotypical basket axon branching in PCL. All together, our data establishes a direct link between extracellular molecular cue SEMA3A and the associated signaling pathway in regulating the specific axon branching pattern of GABAergic interneurons.

#### A Role for SEMA3A in Local GABAergic Axon Branching

We, and others, previously showed that a subcellular gradient of neurofascin-186 located at the AIS of Purkinje cells stabilized basket axon collateral branches at Purkinje soma and the axon hillock where they form the pinceau synapse [17, 43, 44]. Here we further showed that extracellular enrichment of secreted SEMA3A in the PCL instructed the GABAergic axon to branch locally. Extracellular gradient of SEMA3A regulates axon guidance [4], neuronal migration [45], and neuronal polarity [46]. The formation of SEMA3A gradient was mainly suggested based on known mRNA expression patterns [47]. Here we showed local enrichment of SEMA3A as a protein using the specific signal-amplification approach PLA [48]. The enrichment of SEMA3A in the PCL could be explained by the fact that SEMA3A contains a basic region at the carboxyl terminal that may attach to cell membranes or extracellular matrix (ECM), impeding diffusion through the extracellular space [49, 50]. Interesting, SEMA3A interacts with proteoglycans in the ECM or through vesicle matrix that retains secreted SEMA3A

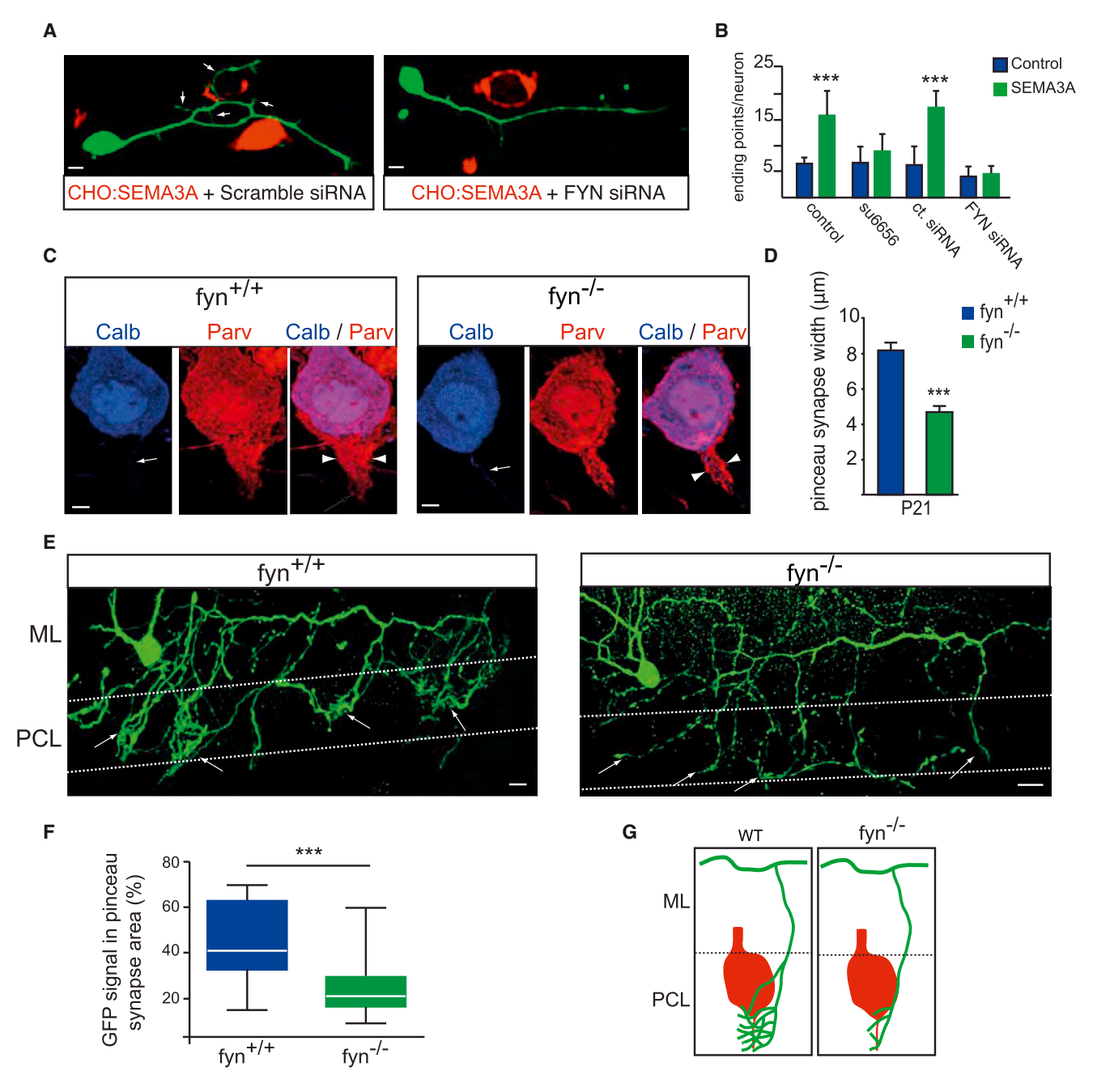


Figure 6. Reduced Layer-Specific Basket Axon Branching in FYN<sup>-/-</sup> Cerebellar Cortex

- (A) Examples of GFP-labeled interneurons transfected with siRNA Scramble or siRNA against FYN in SEMA3A condition.
- (B) Quantification of axonal ending points (n = three cultures, 14-20 cells/condition) showed that su6656 or FYN-siRNA inhibited SEMA3A-induced axon branching.
- (C) Sagittal sections of cerebellum from P21 mice immunolabeled with anti-parvalbumin (Parv, red) or anti-calbindin (Calb, green) or merged in both WT and  $fyn^{-/-}$ . Arrows indicate Purkinje axon and arrowhead points to the pinceau synapse width.
- (D) Quantification of pinceau synapse width at the AIS in both WT and  $fyn^{-/-}$  revealed a statistically significant decrease in  $fyn^{-/-}$  at P21 (n = 12–30 from five WT mice and five mutant mice).
- (E) Example of adult single basket cell axon organization visualized with GFP in compound BAC Parv-GFP::  $fyn^{+/+}$  and Parv-GFP::  $fyn^{-/-}$ . Arrows indicate pinceau synapse. Dotted lines represent Purkinje cell layer (PCL). ML, molecular layer.
- (F) Quantification of GFP signal in pinceau synapse area obtained in three independent experiments (shown as means  $\pm$  SEM; n = 19 for  $fyn^{+/+}$ ; n = 25 for  $fyn^{-/-}$ ).
- (G) Schematic representation of  $fyn^{-/-}$ -deficient basket axon branching at the AIS. Scale bars represent 4  $\mu$ m (A and C) or 10  $\mu$ m (E). Error bars represent SEM. \*\*\*p < 0.001; Mann-Whitney test.

at the cell surface in vitro [51]. During the assembly of specific components of the ECM, NF186 links the specialized brevican-containing extracellular matrix [52]. Because Purkinje cells

expressed both NF186 and brevican [53] and NF186 localized exclusively in the PCL [54], a specialized extracellular matrix could be assembled in the PCL. Although there is currently

no evidence that SEMA3A interacted directly with brevican, the specificity of such assembly could provide a base for SEMA3A local enrichment in the PCL. Notably, neuronal responses to SEMA3A were mainly studied for the diffusible protein gradient established in solution or in gel matrices. This is likely different from the in vivo situation, where SEMA3A is presented to the target cell as a bound form, raising the question of whether the bound form of SEMA3A had the same effect on the neuronal partner compared with the diffusible form. We observed that acute application of SEMA3A both in vitro and in vivo triggered the activation of the same signaling pathway. The role of ECM might thus be to regulate the spatial distribution of extracellular signaling molecules. Indeed, binding to ECM allows secreted growth factors to be sturdily maintained at high concentration for focal signaling [55].

#### Local FYN-sGC Signaling Controls Terminal GABAergic Axon Branching

FYN signaling pathways play a critical role in SEMA3A functions underlying apical dendrite guidance [39] and dendritic branching [56] in the cerebral cortex. In fyn-deficient mice, we did not find any defect in the GABAergic interneuron dendritic organization and observed that the overall axon organization, including the main horizontal branch and descending collaterals, were not significantly different from control WT mice, suggesting that the FYN-signaling pathway was not involved in axon guidance and dendritic guidance or branching. On the other end, we observed a strong branching defect of basket cell axon in the PCL. The formation of axonal branches can be achieved in at least three principal ways, by splitting of the growth cone, by outgrowth of a collateral from the axonal shaft, and by terminal arborization [57]. The fact that the collateral branches emerging from the main axonal shaft were not affected by FYN signaling suggests that the specific mode of axonal branching was regulated by different signaling pathways. This observation was supported by the fact that, in the spinal cord, cGMP signaling cascade induced sensory axon bifurcation [58], but collateral formation was not affected [59]. How is the cGMP level controlled to induce local function? In both vertebrates and invertebrates, several studies suggested that membrane-bound guanylyl cyclases (mGCs) [60] were required for bifurcation of axons [59] or motor neuron pathfinding in flies [61]. In Drosophila, sGC was not essential for semaphorin-mediated function, in contrast to mGC Gyc76c [61]. Thus, one could hypothesize that local increase in cGMP levels was necessary. Consistently, our data showed that SEMA3A triggered cGMP production by recruiting sGC locally at the plasma membrane. sGC localizes to plasma membrane in rat neurons but also in other tissue, like rat vascular endothelial cells or human and rat skeletal myocytes [40, 62, 63]. The importance of this subcellular location and the mechanism involved in the sGC trafficking are at present not known. Here, our findings revealed a novel form of cGMP production at the membrane by recruiting sGC through local protein-protein interaction. Using coimmuprecipitation and PLA experiments, our study demonstrated that FYN phosphorylated and interacted with the  $\beta$ 1 subunit of sGC at the plasma membrane. To this end, FYN phosphorylated the β1 subunit on Y192, which unfolded a SH2 docking site and favored FYN/β1pY192 heterocomplex formation. These findings strongly suggest a role of FYN in sGC trafficking, as suggested by other reports showing that FYN influences the localization and trafficking of other proteins in a phosphorylation-dependent manner [64, 65]. Furthermore, in

GABAergic interneurons, our data supported a role for the FYN-dependent trafficking of sGC to the plasma membrane in GABAergic axon branching. Notably, FYN and plexinA1 physically interact in GABAergic interneurons in vivo (the present study), as suggested previously in vitro [39], supporting the idea that local production of cGMP is essential for SEMA3A-mediated function. Thus, activation of FYN represents an elegant mechanism to localize specific cGMP signaling pathways in subcellular compartments within structures, and as such could represent a more general mechanism for cGMP regulation in response to extracellular cues.

#### **Experimental Procedures**

#### **Mutant Mice and Procedure**

The experimental plan was designed according to the European Communities Council Directive and the French law for care and use of experimental animals. SEMA3A-deficient mice were obtained from RIKEN BioResource Center [66]. NRP1 sema-/sema- mice were previously described [23]. FYN-deficient mice were obtained from JAX Mice [67]. Mutant mice were bred to our BAC transgenic mice Gad67-GFP and parvalbumin-GFP (PV-GFP) [17, 18].

#### Immunohistochemistry and Confocal Microscopy

Mice were anesthetized and transcardially perfused with 4% paraformaldehyde. Sections were cut from cerebellum using a vibratome (Leica VT100). Brain sections were blocked and immunostained. For more technical details of the immunohistochemistry and confocal microscopy method, see Supplemental Experimental Procedures.

#### **PLA Technique**

Sagittal sections 30  $\mu m$  thick were cut from cerebellum using cryostat. Experiments were then done according to the manufacturer's instructions (Olink Bioscience). For more technical details of the cryostat PLA method, see Supplemental Experimental Procedures.

#### Double Sholl Analysis

We used an ImageJ plugin that drew ten concentric circles every 10  $\mu$ M from the cell body of the neuron and the CHO cell. The complexity of the axon from the cell body and in proximity to the transfected CHO was compared. A ratio between axonal complexity around the CHO cell and the interneuron soma was calculated.

#### **Quantification of Pinceau Synapses**

A predefined area for analysis of the GFP signal at the AIS was determined by taking the largest size of the morphological feature of the GFP signal from the pinceau synapse among all WT basket cells. This area was then used as the region of interest in the NIH image software and applied at the basket cell axon terminal in compound Parv-GFP WT and FYN-mutant mice, and the mean pixel intensity of the GFP signal was measured. Each genotype was acquired separately and compared to the control experiment acquired on the same day under the same condition.

#### Western Blotting and Coimmunoprecipitation

HEK293T cells or primary culture were lysed with solubilization buffer (HEPES 20 mM, NaCl 150 mM, 1% NP40, 10% glycerol, 4 mg/ml dodecylmatoside), protease inhibitors, and phosphatase inhibitors. Mouse cerebellar tissues were homogenized in solubilization buffer and centrifuged. The supernatants were collected.

#### Purification of the Membrane Fraction

This was carried out with a Mem-PER Eukaryotic Membrane Protein Extraction Kit (Thermo Scientific) according to the manufacturer's instructions.

#### Coimmunoprecipitation

Lysates were incubated with specific antibodies for overnight at 4°C, and protein A Sepharose (GE Healthcare) or protein AG (protein Bio-Adembeads PAG, Ademtech) was added for 1 hr at 4°C. For more technical details about the protein Bio-Adembeads PAG, Ademtech coimmunoprecipitation method, see Supplemental Experimental Procedures.

#### **Dissociated Cultures**

Cerebella from P3 mice were dissected in cold PBS and cultured during 24 hr in 12-well plates at a concentration of 10<sup>3</sup> cells in 1 ml of medium for immunocytochemistry and in 6-well plates at a concentration of 10<sup>6</sup> cells in 2 ml medium for biochemistry experiments.

#### Coculture

For coculture, CHO cells were plated in a 24-well plate containing 18 mm coverslips and coated with polyornithine. After 1 day, the cell was transfected with plasmids using the JetPRIME transfection reagent (PolyPlus). Subsequently, dissociated GABAergic interneurons were plated on the CHO cells (10<sup>5</sup> cells/well). Pharmacological agents or Neuropilin-1 antibody were added 6–8 hr after plating.

#### **Plasmids and Transfection**

HEK293T cells were transfected 1 day after plating with plasmids using the JetPRIME transfection reagent (Polyplus). Plasmid coding for *EGFP*-SEMA3A was a gift from Joost Verhagen. Plasmid coding for FYN was obtained from Addgene. Constitutively active and dominant-negative FYN mutants were produced by changing Tyr528 to Phe and Lys299 to Met, respectively. sGC alpha1 ( $\alpha$ 1), sGC beta1 ( $\beta$ 1), and sGC  $\beta$ 1Y192F were previously described [37].

#### siRNA

Cerebellar GABAergic interneurons were nucleofected (Amaxa, Lonza) with custom small interfering RNA (siRNA) designed against mouse FYN (Eurogentec) or control (scrambled sequence with the same nucleotides) and plated on coated plates overnight.

#### Supplemental Information

Supplemental Information includes five figures and Supplemental Experimental Procedures and can be found with this article online at http://dx.doi.org/10.1016/j.cub.2013.04.007.

#### Acknowledgments

We thank W. Müller-Esterl, K. Wagner, and S. Oess for phosphospecific antiserum to β1pY192 and sGC-β1 plasmids. We thank the Montpellier RIO Imaging facility, especially J. Cau and N. Lautredou. We are grateful to L. Fagni and J. Bockaërt for their critical reading of the manuscript. F.A. was supported by the Human Frontier Science Program Organization (CDA-0015-2006-C) and INSERM-AVENIR program. F.A. was also supported by the Fondation Fyssen, Fédération pour la recherche sur le cerveau (FRC), Fondation pour la recherche Médicale (FRM), and ANR (ANR-08-JCJC-0044).

Received: November 26, 2012 Revised: March 1, 2013 Accepted: April 2, 2013 Published: April 18, 2013

#### References

- Benson, D.L., Colman, D.R., and Huntley, G.W. (2001). Molecules, maps and synapse specificity. Nat. Rev. Neurosci. 2, 899–909.
- Raper, J., and Mason, C. (2010). Cellular strategies of axonal pathfinding. Cold Spring Harb. Perspect. Biol. 2, a001933.
- Sanes, J.R., and Yamagata, M. (2009). Many paths to synaptic specificity. Annu. Rev. Cell Dev. Biol. 25, 161–195.
- Tessier-Lavigne, M., and Goodman, C.S. (1996). The molecular biology of axon guidance. Science 274, 1123–1133.
- Williams, M.E., de Wit, J., and Ghosh, A. (2010). Molecular mechanisms of synaptic specificity in developing neural circuits. Neuron 68, 9–18.
- O'Leary, D.D., Bicknese, A.R., De Carlos, J.A., Heffner, C.D., Koester, S.E., Kutka, L.J., and Terashima, T. (1990). Target selection by cortical axons: alternative mechanisms to establish axonal connections in the developing brain. Cold Spring Harb. Symp. Quant. Biol. 55, 453–468.
- Yamahachi, H., Marik, S.A., McManus, J.N., Denk, W., and Gilbert, C.D. (2009). Rapid axonal sprouting and pruning accompany functional reorganization in primary visual cortex. Neuron 64, 719–729.
- Sanes, J.R., and Lichtman, J.W. (1999). Can molecules explain longterm potentiation? Nat. Neurosci. 2, 597–604.

- Kawaguchi, Y., and Kubota, Y. (1993). Correlation of physiological subgroupings of nonpyramidal cells with parvalbumin- and calbindinD28kimmunoreactive neurons in layer V of rat frontal cortex. J. Neurophysiol. 70, 387–396.
- Thomson, A.M., and Bannister, A.P. (2003). Interlaminar connections in the neocortex. Cereb. Cortex 13, 5–14.
- Wang, Y., Gupta, A., Toledo-Rodriguez, M., Wu, C.Z., and Markram, H. (2002). Anatomical, physiological, molecular and circuit properties of nest basket cells in the developing somatosensory cortex. Cereb. Cortex 12, 395–410.
- Tamás, G., Lorincz, A., Simon, A., and Szabadics, J. (2003). Identified sources and targets of slow inhibition in the neocortex. Science 299, 1902–1905.
- Tamás, G., Buhl, E.H., Lörincz, A., and Somogyi, P. (2000). Proximally targeted GABAergic synapses and gap junctions synchronize cortical interneurons. Nat. Neurosci. 3, 366–371.
- Palay, S.L., and Chan-Palay, V., eds. (1974). Cerebellar Cortex: Cytology and Organization (New York: Springer-Verlag).
- Karube, F., Kubota, Y., and Kawaguchi, Y. (2004). Axon branching and synaptic bouton phenotypes in GABAergic nonpyramidal cell subtypes. J. Neurosci. 24, 2853–2865.
- Sotelo, C. (2008). Development of "Pinceaux" formations and dendritic translocation of climbing fibers during the acquisition of the balance between glutamatergic and gamma-aminobutyric acidergic inputs in developing Purkinje cells. J. Comp. Neurol. 506, 240–262.
- Ango, F., di Cristo, G., Higashiyama, H., Bennett, V., Wu, P., and Huang, Z.J. (2004). Ankyrin-based subcellular gradient of neurofascin, an immunoglobulin family protein, directs GABAergic innervation at purkinje axon initial segment. Cell 119, 257–272.
- Ango, F., Wu, C., Van der Want, J.J., Wu, P., Schachner, M., and Huang, Z.J. (2008). Bergmann glia and the recognition molecule CHL1 organize GABAergic axons and direct innervation of Purkinje cell dendrites. PLoS Biol. 6. e103.
- Rabacchi, S.A., Solowska, J.M., Kruk, B., Luo, Y., Raper, J.A., and Baird, D.H. (1999). Collapsin-1/semaphorin-III/D is regulated developmentally in Purkinje cells and collapses pontocerebellar mossy fiber neuronal growth cones. J. Neurosci. 19, 4437–4448.
- Catalano, S.M., Messersmith, E.K., Goodman, C.S., Shatz, C.J., and Chédotal, A. (1998). Many major CNS axon projections develop normally in the absence of semaphorin III. Mol. Cell. Neurosci. 11, 173–182.
- He, Z., and Tessier-Lavigne, M. (1997). Neuropilin is a receptor for the axonal chemorepellent Semaphorin III. Cell 90, 739–751.
- Kolodkin, A.L., Levengood, D.V., Rowe, E.G., Tai, Y.T., Giger, R.J., and Ginty, D.D. (1997). Neuropilin is a semaphorin III receptor. Cell 90, 753–762.
- Gu, C., Rodriguez, E.R., Reimert, D.V., Shu, T., Fritzsch, B., Richards, L.J., Kolodkin, A.L., and Ginty, D.D. (2003). Neuropilin-1 conveys semaphorin and VEGF signaling during neural and cardiovascular development. Dev. Cell 5, 45–57.
- Sanes, J.R., and Yamagata, M. (1999). Formation of lamina-specific synaptic connections. Curr. Opin. Neurobiol. 9, 79–87.
- Marshak, S., Nikolakopoulou, A.M., Dirks, R., Martens, G.J., and Cohen-Cory, S. (2007). Cell-autonomous TrkB signaling in presynaptic retinal ganglion cells mediates axon arbor growth and synapse maturation during the establishment of retinotectal synaptic connectivity. J. Neurosci. 27. 2444–2456.
- Song, H., Ming, G., He, Z., Lehmann, M., McKerracher, L., Tessier-Lavigne, M., and Poo, M. (1998). Conversion of neuronal growth cone responses from repulsion to attraction by cyclic nucleotides. Science 281, 1515–1518.
- Houchin-Ray, T., Zelivyanskaya, M., Huang, A., and Shea, L.D. (2009). Non-viral gene delivery transfection profiles influence neuronal architecture in an in vitro co-culture model. Biotechnol. Bioeng. 103, 1023–1032
- Tang, F., and Kalil, K. (2005). Netrin-1 induces axon branching in developing cortical neurons by frequency-dependent calcium signaling pathways. J. Neurosci. 25, 6702–6715.
- Goodman, C.S. (1996). Mechanisms and molecules that control growth cone guidance. Annu. Rev. Neurosci. 19, 341–377.
- Campbell, D.S., Regan, A.G., Lopez, J.S., Tannahill, D., Harris, W.A., and Holt, C.E. (2001). Semaphorin 3A elicits stage-dependent collapse, turning, and branching in Xenopus retinal growth cones. J. Neurosci. 21, 8538–8547.

- Vles, J.S., de Louw, A.J., Steinbusch, H., Markerink-van Ittersum, M., Steinbusch, H.W., Blanco, C.E., Axer, H., Troost, J., and de Vente, J. (2000). Localization and age-related changes of nitric oxide- and ANP-mediated cyclic-GMP synthesis in rat cervical spinal cord: an immunocytochemical study. Brain Res. 857, 219–234.
- van Staveren, W.C., Markerink-van Ittersum, M., Steinbusch, H.W., Behrends, S., and de Vente, J. (2005). Localization and characterization of cGMP-immunoreactive structures in rat brain slices after NO-dependent and NO-independent stimulation of soluble guanylyl cyclase. Brain Res. 1036, 77–89.
- Desai, C.J., Sun, Q., and Zinn, K. (1997). Tyrosine phosphorylation and axon guidance: of mice and flies. Curr. Opin. Neurobiol. 7, 70–74.
- Robles, E., Woo, S., and Gomez, T.M. (2005). Src-dependent tyrosine phosphorylation at the tips of growth cone filopodia promotes extension. J. Neurosci. 25, 7669–7681.
- Tuttle, R., and O'Leary, D.D. (1998). Neurotrophins rapidly modulate growth cone response to the axon guidance molecule, collapsin-1. Mol. Cell. Neurosci. 11, 1-8.
- Obenauer, J.C., Cantley, L.C., and Yaffe, M.B. (2003). Scansite 2.0: Proteome-wide prediction of cell signaling interactions using short sequence motifs. Nucleic Acids Res. 31, 3635–3641.
- Meurer, S., Pioch, S., Gross, S., and Müller-Esterl, W. (2005). Reactive oxygen species induce tyrosine phosphorylation of and Src kinase recruitment to NO-sensitive guanylyl cyclase. J. Biol. Chem. 280, 33149–33156.
- Resh, M.D. (1998). Fyn, a Src family tyrosine kinase. Int. J. Biochem. Cell Biol. 30, 1159–1162.
- Sasaki, Y., Cheng, C., Uchida, Y., Nakajima, O., Ohshima, T., Yagi, T., Taniguchi, M., Nakayama, T., Kishida, R., Kudo, Y., et al. (2002). Fyn and Cdk5 mediate semaphorin-3A signaling, which is involved in regulation of dendrite orientation in cerebral cortex. Neuron 35, 907–920.
- Zabel, U., Kleinschnitz, C., Oh, P., Nedvetsky, P., Smolenski, A., Müller, H., Kronich, P., Kugler, P., Walter, U., Schnitzer, J.E., and Schmidt, H.H. (2002). Calcium-dependent membrane association sensitizes soluble guanylyl cyclase to nitric oxide. Nat. Cell Biol. 4, 307–311.
- Bellucci, A., Navarria, L., Falarti, E., Zaltieri, M., Bono, F., Collo, G., Spillantini, M.G., Missale, C., and Spano, P. (2011). Redistribution of DAT/α-synuclein complexes visualized by "in situ" proximity ligation assay in transgenic mice modelling early Parkinson's disease. PLoS ONE 6, e27959.
- Stepanyants, A., Tamás, G., and Chklovskii, D.B. (2004). Class-specific features of neuronal wiring. Neuron 43, 251–259.
- Zonta, B., Desmazieres, A., Rinaldi, A., Tait, S., Sherman, D.L., Nolan, M.F., and Brophy, P.J. (2011). A critical role for Neurofascin in regulating action potential initiation through maintenance of the axon initial segment. Neuron 69, 945–956.
- Buttermore, E.D., Piochon, C., Wallace, M.L., Philpot, B.D., Hansel, C., and Bhat, M.A. (2012). Pinceau organization in the cerebellum requires distinct functions of neurofascin in Purkinje and basket neurons during postnatal development. J. Neurosci. 32, 4724–4742.
- Chen, G., Sima, J., Jin, M., Wang, K.Y., Xue, X.J., Zheng, W., Ding, Y.Q., and Yuan, X.B. (2008). Semaphorin-3A guides radial migration of cortical neurons during development. Nat. Neurosci. 11, 36–44.
- Polleux, F., Morrow, T., and Ghosh, A. (2000). Semaphorin 3A is a chemoattractant for cortical apical dendrites. Nature 404, 567–573.
- 47. Zhao, H., Maruyama, T., Hattori, Y., Sugo, N., Takamatsu, H., Kumanogoh, A., Shirasaki, R., and Yamamoto, N. (2011). A molecular mechanism that regulates medially oriented axonal growth of upper layer neurons in the developing neocortex. J. Comp. Neurol. 519, 834–848.
- Weibrecht, I., Leuchowius, K.J., Clausson, C.M., Conze, T., Jarvius, M., Howell, W.M., Kamali-Moghaddam, M., and Söderberg, O. (2010). Proximity ligation assays: a recent addition to the proteomics toolbox. Expert Rev. Proteomics 7, 401–409.
- Kolodkin, A.L. (1996). Growth cones and the cues that repel them. Trends Neurosci. 19, 507–513.
- Nakamura, F., Kalb, R.G., and Strittmatter, S.M. (2000). Molecular basis of semaphorin-mediated axon guidance. J. Neurobiol. 44, 219–229.
- De Wit, J., De Winter, F., Klooster, J., and Verhaagen, J. (2005).
  Semaphorin 3A displays a punctate distribution on the surface of neuronal cells and interacts with proteoglycans in the extracellular matrix. Mol. Cell. Neurosci. 29, 40–55.
- Hedstrom, K.L., Xu, X., Ogawa, Y., Frischknecht, R., Seidenbecher, C.I., Shrager, P., and Rasband, M.N. (2007). Neurofascin assembles a

- specialized extracellular matrix at the axon initial segment. J. Cell Biol. 178, 875-886.
- Bekku, Y., Saito, M., Moser, M., Fuchigami, M., Maehara, A., Nakayama, M., Kusachi, S., Ninomiya, Y., and Oohashi, T. (2012). Bral2 is indispensable for the proper localization of brevican and the structural integrity of the perineuronal net in the brainstem and cerebellum. J. Comp. Neurol. 520, 1721–1736.
- Zhou, D., Lambert, S., Malen, P.L., Carpenter, S., Boland, L.M., and Bennett, V. (1998). AnkyrinG is required for clustering of voltage-gated Na channels at axon initial segments and for normal action potential firing. J. Cell Biol. 143, 1295–1304.
- Park, J.E., Keller, G.A., and Ferrara, N. (1993). The vascular endothelial growth factor (VEGF) isoforms: differential deposition into the subepithelial extracellular matrix and bioactivity of extracellular matrix-bound VEGF. Mol. Biol. Cell 4, 1317–1326.
- Morita, A., Yamashita, N., Sasaki, Y., Uchida, Y., Nakajima, O., Nakamura, F., Yagi, T., Taniguchi, M., Usui, H., Katoh-Semba, R., et al. (2006). Regulation of dendritic branching and spine maturation by semaphorin3A-Fyn signaling. J. Neurosci. 26, 2971–2980.
- Schmidt, H., and Rathjen, F.G. (2010). Signalling mechanisms regulating axonal branching in vivo. Bioessays 32, 977–985.
- Zhao, Z., and Ma, L. (2009). Regulation of axonal development by natriuretic peptide hormones. Proc. Natl. Acad. Sci. USA 106, 18016–18021.
- Schmidt, H., Stonkute, A., Jüttner, R., Koesling, D., Friebe, A., and Rathjen, F.G. (2009). C-type natriuretic peptide (CNP) is a bifurcation factor for sensory neurons. Proc. Natl. Acad. Sci. USA 106, 16847– 16852.
- Wedel, B., and Garbers, D. (2001). The guanylyl cyclase family at Y2K. Annu. Rev. Physiol. 63, 215–233.
- Ayoob, J.C., Yu, H.H., Terman, J.R., and Kolodkin, A.L. (2004). The Drosophila receptor guanylyl cyclase Gyc76C is required for semaphorin-1a-plexin A-mediated axonal repulsion. J. Neurosci. 24, 6639– 6649.
- Linder, A.E., McCluskey, L.P., Cole, K.R., 3rd, Lanning, K.M., and Webb, R.C. (2005). Dynamic association of nitric oxide downstream signaling molecules with endothelial caveolin-1 in rat aorta. J. Pharmacol. Exp. Ther. 314, 9–15.
- Russwurm, M., Wittau, N., and Koesling, D. (2001). Guanylyl cyclase/ PSD-95 interaction: targeting of the nitric oxide-sensitive alpha2beta1 guanylyl cyclase to synaptic membranes. J. Biol. Chem. 276, 44647– 44652.
- Shima, T., Okumura, N., Takao, T., Satomi, Y., Yagi, T., Okada, M., and Nagai, K. (2001). Interaction of the SH2 domain of Fyn with a cytoskeletal protein, beta-adducin. J. Biol. Chem. 276, 42233–42240.
- 65. Usardi, A., Pooler, A.M., Seereeram, A., Reynolds, C.H., Derkinderen, P., Anderton, B., Hanger, D.P., Noble, W., and Williamson, R. (2011). Tyrosine phosphorylation of tau regulates its interactions with Fyn SH2 domains, but not SH3 domains, altering the cellular localization of tau. FEBS J. 278, 2927–2937.
- Taniguchi, M., Yuasa, S., Fujisawa, H., Naruse, I., Saga, S., Mishina, M., and Yagi, T. (1997). Disruption of semaphorin III/D gene causes severe abnormality in peripheral nerve projection. Neuron 19, 519–530.
- Stein, P.L., Lee, H.M., Rich, S., and Soriano, P. (1992). pp59fyn mutant mice display differential signaling in thymocytes and peripheral T cells. Cell 70, 741–750.